Structural investigation of austenitic stainless steel layers obtained by laser surface alloying

R. I. ZAMFIR*, E. POPOVICI[a], F. MICULESCU, M. DANILA[b], A. PARAU
Department of Metallic Materials Science, Physical Metallurgy, Science and Engineering Materials Faculty, University Politehnica of Bucharest, 313 Splaiul Independentei, Bucharest, 060042, Romania,
[a]*National Institute for Laser, Plasma and Radiation Physics, 409 Atomistilor Street, Magurele Bucharest, 077125, Romania*
[b]*National Institute for R&D in Microtechnologies, IMT Bucharest, 126 A, Erou Iancu Nicolae Blvd., Voluntari, Ilfov county, Romania*

The goal of this study is to characterize the coatings obtained by laser surface alloying of low-alloy steel with 316L stainless steel powder. The laser surface alloying (LSA) process was carried out using a pulsed single-mode CO_2 laser (600 W, 200 kHz operation frequency). In order to avoid the sample overheating during irradiation, the samples were cooled in liquid nitrogen. The alloyed layers were characterized by X-ray Diffraction (XRD), scanning electron microscopy (SEM), energy dispersive X-ray (EDX) analysis, and microhardness testing. The layers were compact and homogeneous, with an uniform distribution of Cr, Ni and Mo elements, both at the surface and throughout their depth. EDX analysis revealed that the outer layer has a concentration of alloying elements (Cr, Ni, Mo) corresponding to a ferrito-austenitic stainless steel. These concentrations decreased to the substrate, as a result of the penetration process of the alloying elements from the surface towards the core. XRD analysis revealed nanostructured layers consisting of ferrito-austenite, regardless of the applied power density. Depending on the laser processing parameters, the surface layers exhibited higher hardness values than the untreated samples.

(Received June 7, 2012; accepted April 11, 2013)

Keywords: Laser alloying; Low alloying steel; 316L; Microstructure; Composition; Microhardness

1. Introduction

The laser surface alloying (LSA) process is aiming to improve the surface properties (corrosion and wear resistance) required in certain applications, as automotive, aerospace, and oil industries [1-14].

The LSA process involves the melting of the material till certain depths, the disolution of different alloying elements within it, followed by the rapid cooling and solidification leading to submicrocrystalline or nanocrystalline structures [15], as these types of material present, in general, superior mechanical characteristics [16]. The surface layers produced during this process present different structures and compositions, due to the alloying process, while the treated parts maintain their initial shapes.

The surface properties obtained by LSA process are controlled by the laser power density, as well by the duration of the material-laser beam interaction, determined by the velocity of the irradiated sample. The composition of the deposited alloy and its thickness are determined by the laser parameters (lengthwave, energy per pulse, number and frequency of the pulses), and by the specific method through which the material to be alloyed is fed on the sample surface (powder, paste pre-deposited layers etc).

There are several studies reported in the literature on LSA treatments done on high alloy stainless steels [1, 2, 4] or low alloy steels [5, 12], aiming to increase the microhardness [1, 2], the wear resistance [1, 3-5], and the corrosion resistance [1, 6-11]. In these works, different powders were used such as Cr, Ni, Mo, C, W, and Al, in various proportions [2, 5, 11], as well as mixtures of these elements [1]. The results obtained so far showed that, depending on the technological parameters of the LSA process, different structures and compositions were obtained for the layers, ensuring the expected characteristics [1, 2, 5, 12, 14].

The goal of the present study is to characterize the coatings obtained by laser surface alloying of low-alloy steel with 316L stainless steel powder. Different concentrations of the alloying elements in the deposited layers were obtained by varying the sample velocity and the laser beam power density.

Due to the small volume of our samples, we found that material transformations appear in the laser melted zones, even for single pass iradiation. A rapid cooling device with liquid nitrogen was used [17], which ensured reproducible cooling conditions, in order to produce a nanocrystalline structure of the alloyed layer.

2. Experimental procedure

The samples consisted of discs (25 mm in diameter, 10 mm thick) made of hardened and tempered low alloy

steel, with a hardness value of 206 $HV_{0.025}$. The chemical composition of the steel was determined by optical emission spectrometry on a spectrometer type SPECTROMAXxM X LMM 04, using an analytical program Fe-10-M for low alloying steels, and is presented in Table 1.

The chemical composition of the 316L stainless steel powder (Anval Inc., Sweden) used for the LSA process, with grain dimension in the range 10 - 40 μm, is presented in Table 2.

The powder was applied on the sample surface durring iradiation, with a powder dosing device connected to an argon gas bottle, delivering a constant mass flow of 5g/min. special device and cooled in liquid nitrogen. The device used for sample cooling, presented in Fig. 1, allows a large volume to be cooled by liquid nitrogen, in order to ensure proper, similar and reproducible cooling conditions for all the iradiated samples.

Table 1. Chemical composition of the steel.

Element	C	Mn	Si	Cr	Ni	Cu	S	P	Mo	As	Al	N	Fe
at. %	0.309	1.06	1.35	0.890	0.145	0.179	<0.0001	<0.0005	0.023	0.02	0.02	0.02	95.9

Table 2. Chemical composition of 316L powder.

Element	C	Si	Ni	Cr	Mo	Mn	Fe
at. %	0.02	0.8	13	17	2.2	0.2	balance

Table 3. LSA process parameters

Sample	I_{Si} (kW/cm^2)	v (mm/s)	$HV_{0.025}$
S1	72.65	5.0	718
S2	72.65	6.5	653
S3	72.65	8.0	548
S4	87.29	5.0	688
S5	87.29	6.5	603
S6	87.29	8.0	483

LSA was carried out using a single mode, 600 W pulsed (200 kHz) CO_2 laser. The power density variation on the treated surface was obtained by modifying the dimension of the focal spot on the iradiated surface. We have obtained single trace superficial alloyed bands, with a lengh of 25 mm, and a width determined by the laser spot diameter (~ 1.0 and 1.2 mm).

The LSA process was carried out under a protective argon atmosphere, at the two different power densities: I_{S1} = 72.65 kW/cm^2 and I_{S2} = 87.29 kW/cm^2, coresponding to the two diameters of the focal spots: d_1=1.2 mm and d_2=1.0 mm.

The module used for the sample positioning/movement ensured the controlled movement in a plane in front of the laser beam. Three different sample velocities „v" were selected for investigation: 5 mm/s, 6.5 mm/s and 8 mm/s, for each power density delivered to the samples, as presented in Table 3.

In order to increase the absorption of the laser radiation into the treated surfaces, the samples were previously sprayed with a black paint (type 584909C, RAL 9005 from Motip Dupli GmbH). The coating thickness was about a few μm. It was not observed any alteration of the alloyed layer due to this paint. To avoid sample overheating during irradiation and to ensure a high-speed cooling, the samples were positioned in a

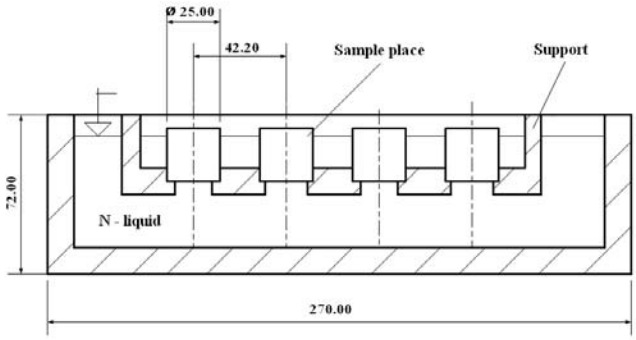

Fig.1. Samples' cooling holderusing liquid nitrogen.

The cross-section of the irradiated samples were analyzed by optical microscopy, using a Reichert microscope UnivaR with automatic inspection table.

The layers' microhardness was determined through Vickers method, for 0.25 N load, with a Micro-Vickers Hardness tester, model 400 – DTS/2.

The samples' morphology and the microstructures were analyzed by scanning electron microscopy (SEM) using a Fei Inspect F microscope. The layer composition was studied by EDX analysis, using a scanning electron microscope (Philips XL 30 ESEM TMP).

The phase composition and the average crystallite size were determined by X-ray diffraction method, using Cu K_α radiation at 2° grazing incidence, and a paralell beam setup (multilayer mirror only), on a Rigaku SmartLab equipment with a 9 kW rotating anode. The XRD system used automated data acquisition software and specialised analysis software packages (PDXL complete package for Rietveld method and the Debye-Scherrer relation).

3. Results and discussion

3.1. Microstructure and morphology

Cross-sectional optical images of a laser alloyed layer (sample S1) is showed in Fig. 2. It can be distinguished the

molten zone of the alloyed material (with a lenticular shape) and a transition region (the thermal influence zone) between the layer and the substrate. The fine microstructure in the alloying layer is due to the high cooling rate which refined the grains. At interface between the layer and the substrate, a proper microstructural and metallurgical bond transition can be observed. For this sample, the layer thickness in the middle of the alloyed layer is ~ 230 μm.

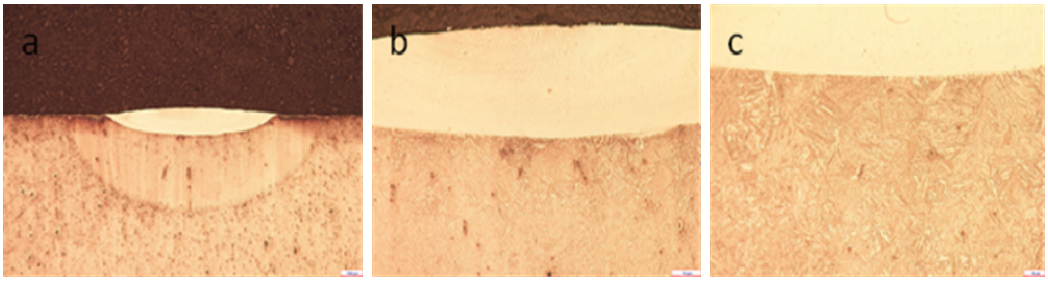

Fig. 2. Optical image of a laser alloyed layer in S1 sample: a - laser alloyed layer; b - amplified image of surface alloying zone; c - amplified image of interface between alloying zone and thermal influence substrate.

As expected, the layer thickness δ was found to depend on both laser power density I_{Si} and sample velocity v (Fig. 3).

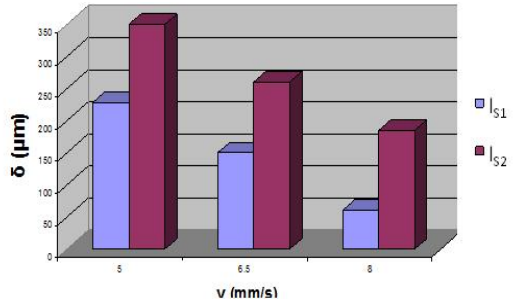

Fig. 3. The layer thickness δ vs laser power density and sample velocity.

The microstructural characteristics of the layers were investigated using scanning electron microscopy. Fig. 4 shows the cross-sectional SEM micrographs of two selected samples (S2 and S5). The SEM images revealed the structural homogeneity and the absence of defects (pores, voids, cracks) both in the alloyed layers and in the thermal influence zones. It is important to notice the fine grained structures of the layers, as well as the specific appeareance of mixed ferrito-austenitic structures. One may also observe that the increasing laser power resulted in a more refined microstructure, as seen when comparing Fig. 4 c and d with Fig. 4 a and b.

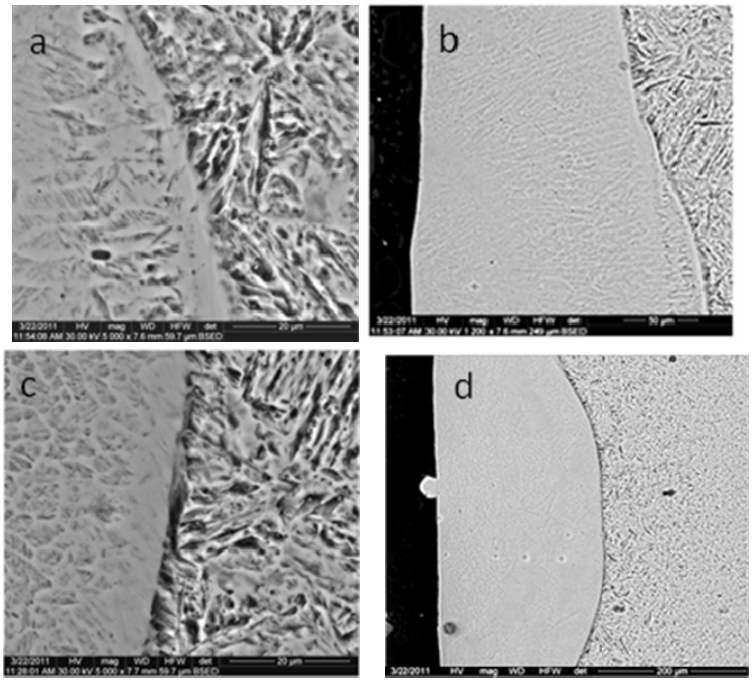

Fig. 4. Cross-sectional SEM micrographs of laser alloyed layers: a - S1, 5000 x; b - S1, 1200 x; c - S2, 5000 x; d - S2, 1200 x.

The surface morphology of the layers was examined by SEM. Fig. 5 shows an example of a SEM image of a layer surface (S2), revealing the presence of nanodimensional formations.

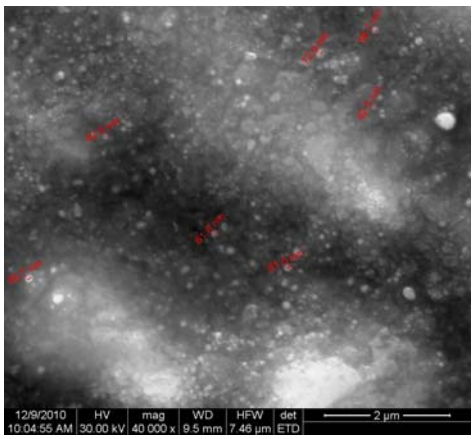

Fig. 5. SEM micrograph of a layer surface (sample S2)

3.2. Elemental composition, crystalline structure and layer microhardness

The elemental composition depth profiles in the alloying layers were obtained by EDX quantitative analysis.

A typical EDX spectrum (sample S5) is shown in Fig. 6, while two examples of EDX depth profiles (samples S2 and S4) are given in Fig. 7.

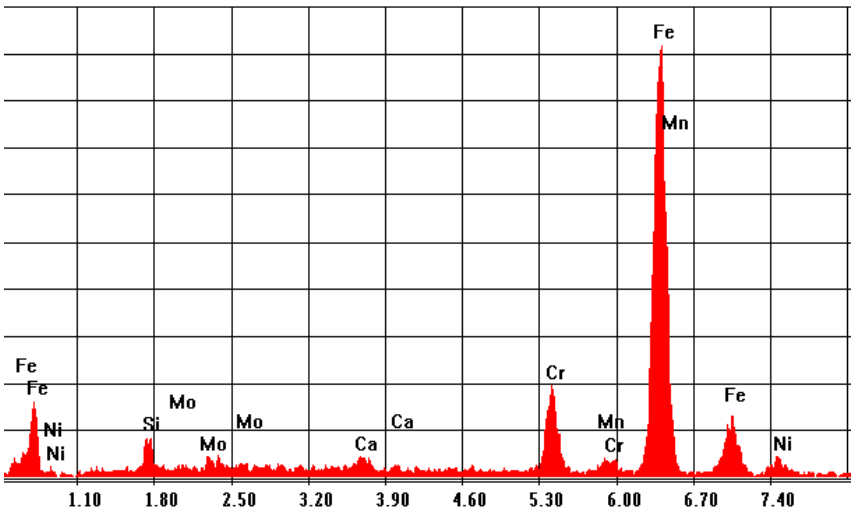

Fig. 6. EDX spectrum on the S5 sample surface.

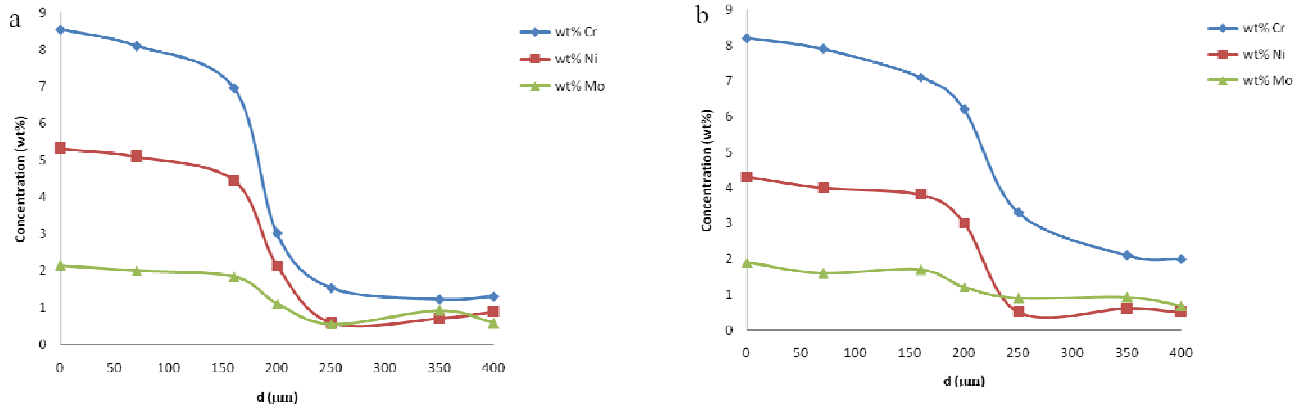

Fig. 7. EDX depth profiles of Cr, Ni and Mo for laser alloyed layers; a - sample S2; b - sample S4.

For both samples, the atomic concentrations of the alloying elements Cr, Ni, and Mo are almost constant in the alloying layer depth. In the thermal influence zone, these concentrations markedly decrease towards the substrate, due to the slow diffusion of the alloying elements into the sample bulk. As expected, for the sample prepared at a higher laser power density (sample S4), a higher penetration depths of Cr, Ni and Mo are observed, which indicate an increased thickness of the modified surface layer.

In order to verify the chemical homogeneity of the layers, the element distribution mapping on the layer surfaces was performed. As an example, Fig. 8 shows a SEM image of a layer surface (sample S5) and the EDX mapping of Cr, revealing the uniform distribution of this element.

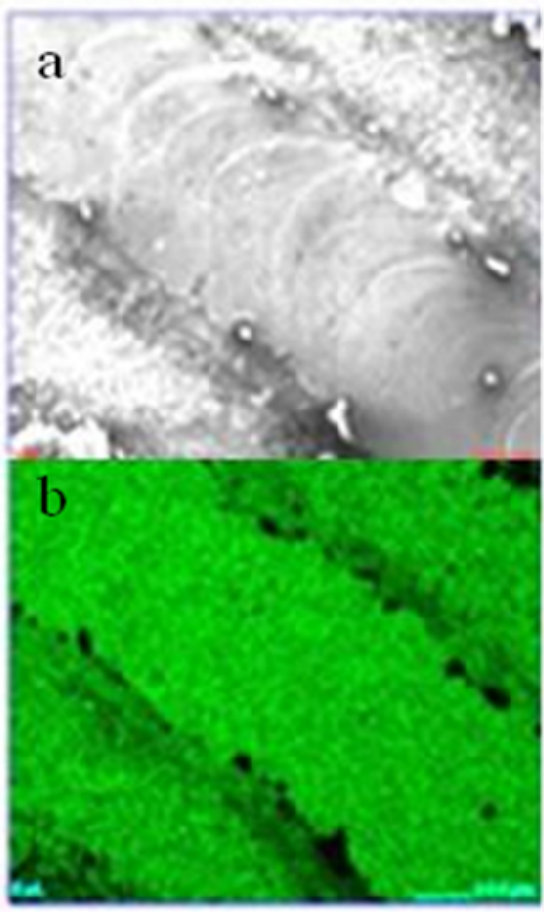

Fig. 8. SEM image of S5 surface (a), with the Cr distribution mapping (b)

Phase compositions, cell parameters and crystallite sizes of the investigated layers were determined by X-ray structural analysis. The diffraction patterns of two selected samples (S1 and S2), prepared at the same sample velocity (6.5 mm/s) but different laser power densities (72.65 kW/cm^2 and 87.29 kW/cm^2), are presented in Fig. 9.

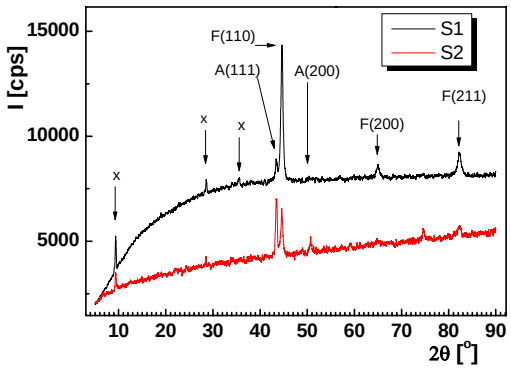

Fig. 9. Diffractions patterns of two laser alloyed layers (sample S1 and S2)

The XRD data indicate the presence of a mixture of a BCC α-Fe ferritic phase and a FCC γ-Fe austenitic phase (the small peaks denoted "x" show the existence of small amounts of unidentified other phases). The cell parameters of the α-Fe phase for the S1 and S2 samples were of 2.8636 Å and 2.876 Å, respectively, slightly larger than the value given in literature (2.860 Å, JCPDS card 87-0722), suggesting the presence of a tensile strain in the alloyed layers. It is interesting to note that the proportion of the austenitic phase significantly incresed as the laser power increased.

The average crystallite size d of both ferritic and austenitic phases were calculated by the Halder-Wagner method (a variant of the Hall-Williamson method). The calculated d values for the austenitic γ-Fe phase were found to be lower than those for the ferritic α-Fe phase. For both detected phases, the crystallite sizes were found to increase with laser power density, from 37.2 nm to 74.9 nm for α-Fe, and from 19.7 nm to 34.1 nm for γ-Fe, at a power density enhancement from 72.65 kW/cm^2 to 87.29 kW/cm^2.

The microhardness depth profiles of the laser alloyed layers were obtained by Vickers microhardness testing. As an example, the microhardness prints on the cross-section of the sample S3 are shown in Fig. 10. The microhardness values measured at a depth of 100 μm are summarised in Table 1. It can be seen that the layer microhardness increased with decreasing the sample velocity and the laser power density, being always higher than that of the untreated samples (206 $HV_{0.025}$).

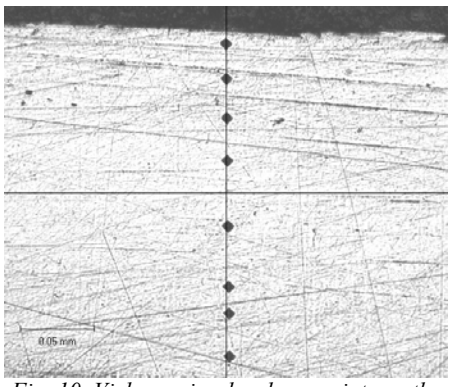

Fig. 10. Vickers microhardness prints on the cross-section of the sample S3

4. Conclusions

The different irradiation regimes in a LSA process studied in the present work aimed to improve the surface properties of a low alloy steel by laser surface alloying with a 316L stainless steel powder, the treated samples being cooled during the process with liquid nitrogen.

LSA layers obtained were characterized by optical microscopy, hardness testing, scanning electron microscopy (SEM), energy dispersive X-ray spectroscopy (EDX), and X-ray diffraction (XRD). The resulted layers were compact and homogeneous, with an uniform distribution of Cr, Ni and Mo.

The elemental analysis carried out on the samples cross-sections revealed that the laser alloyed layers presented Cr, Ni and Mo concentration values corresponding to a ferrito-austenitic stainless steel. The in-depth concentration values decreased towards the underlayer, due to different diffusion coefficients of the alloying elements.

The treated samples presented higher hardness values than the untreated samples, regardless of the power density and at the sample speed.

The XRD analysis revealed nano-scale ferrito-austenitic structures of the investigated layers.

Acknowledgement

"Authors recognise financial support from the European Social Fund through POSDRU/89/1.5/S/54785 project : "Postdoctoral Program for Advanced Research in the field of nanomaterials".

References

[1] John C. Betts, Journal of Materials Processing Technology, **209**(21), 5229 (2009).
[2] Z. Brytan, M. Bonek, L.A. Dobrzański, Journal of Achievements in Materials and manufacturing Engineering, **40**, 70 (2010).
[3] Gui-fang Sun, Yong-kang Zhang, Chang-sheng Liu, Kai-yu Luo, Xing-qi Tao and Peng Li, Materials & Design, **31**, 2737 (2010).
[4] Girish R. Desale, C.P. Paul, B.K. Gandhi, S.C. Jain, Wear, vol. **266,**. 975 (2009).
[5] Xin Tong , Fu-hai Li, Min Kuang, Wen-you Ma, Xing-chi Chen, Min Liu, Applied Surface Science, **258**, 3214 (2012).
[6] K.A. Qureshi, N. Hussain, J.I. Akhter, N. Khan, A. Hussain, Materials Letters, **59**, 719 (2005).
[7] Liang Young and LI Ruiguo, Chin. J. Met. Sci. Technol,. **8** 313 (1992).
[8] M. Szkodo, Journal of Materials Processing Technology, **162,** 410 (2005).
[9] A. Hussain, I. Ahmad, A.H. Hamdani, A. Nussair, S. Shahdin, Mater. Lett., **59,** 719 (2005).
[10] Jianhua Yao, Liang Wang, Qunli Zhang, Fanzhi Kong, Chenghua Lou, Zhijun Chen, Optics & Laser Technology, **40**, 838 (2008).
[11] B. Abdolahi**,** H.R. Shahverdi**,** M.J. Torkamany**,** M. Emami**,** Applied Surface Science, **257**, 9921 (2011).
[12] M. Szkodo, 13th International Scientific Conference on Achievements in Mechanical and Engineering, 16th -19th May 2005, Gliwice-Wista, Poland, pp. 643-646
[13] Tian Fu, Todd E. Sparks, Frank Liou, Zhiqiang Fan, Jianzhong Ruan, Joseph Newkirk, Syamala R. Pulugurtha, Hsin-Nan Chou, Air Force Research Laboratory, STINFO COPY, approved for public distribution, available online MARCH 2010.
[14] T. Glaeser, S. Bausch, C. Ruset, E. Grigore, T. Craciunescu, I. Tiseanu, Plasma Process. Polym. **6**-S1, S291 (2009),
[15] Yoshiaki Morisada, Hidetoshi Fujii, Tadashi Mizuno, Genryu Abe, Toru Nagaoka, Masao Fukusumi, Surface & Coatings Technology, **205,** 3397 (2011).
[16] A.I. Gusev, „Nanomaterialy, nanostruktury, nanotekhnologii", Moscow, Fizmatlit, 2005
[17] R. Zamfir, doctoral thesis „Contributions to the study of the structural and the exploitation characteristics of superficial laser treated austenitic stainless steels", University Politehnica of Bucharest, 2009.

*Corresponding author: ralucaza@yahoo.com